

Cascade Complexes of an Octaaza Cryptand: Co-ordinated Azide with Linear M–NNN–M Geometry*

Michael G. B. Drew,^a Josie Hunter,^b Debbie J. Marrs,^{b,c} Jane Nelson^{b,c} and Charlie Harding^c

^a Chemistry Department, The University, Whiteknights, Reading RG6 2AD, UK

^b School of Chemistry, Queens University, Belfast BT9 5AG, UK

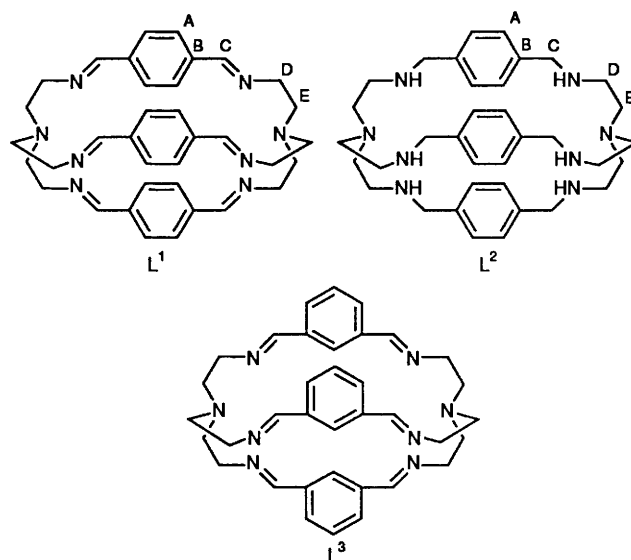
^c Chemistry Department, The Open University, Milton Keynes MK7 6AA, UK

The octaamino cryptand, L², obtained by tetrahydroborate reduction of the [2+3] condensation product of tris(2-ethylamino)amine with terephthalaldehyde, acts as a host for pairs of protons or first-series transition-metal cations. An X-ray crystallographic structure determination of [H₄L²]⁴⁺ reveals a pair of protons held at opposite ends of the molecule by strong intramolecular hydrogen bonding of each proton to two of the amino nitrogen atoms. Pairs of transition-metal cations co-ordinated to the amino N-donors accommodate mono- and tri-atomic bridging ligands, such as OH⁻ or imidazolate, generating weak to moderate antiferromagnetic interaction. Dicopper(II) μ -azido complexes have been prepared where the combination of a large zero-field splitting in the ESR spectrum and a near Curie-law dependence of magnetic susceptibility on temperature seems to suggest a triplet ground state. Together with other unusual spectroscopic properties of the bridging azide group, this is believed to derive from a near-linear alignment of the M–NNN–M assembly.

Polyaza cryptands incorporating sp³ donors have been the subject of extensive study by Lehn and co-workers.^{1,2} In comparison with polyether-linked macrobicycles, they show enhanced co-ordinating power for transition-metal ions, permitting the encapsulation of a pair of ions disposed along the axis of a binuclear complex. In principle, where the macrobicyclic ligand provides a pair of N₄ donor sites, co-ordinative unsaturation offers the opportunity to bind a bridging ligand between the metal sites as has been done for macrocyclic complexes.³ In practice, few examples of such systems have been reported to date.

We have been interested for some time^{4,5} in magnetic interactions mediated by bridging ligands held between transition-metal ions in macrocyclic ligands, and now wish to extend this study to the investigation of dinuclear cryptates, which offer superior insulation of the interacting paramagnets, reducing the importance of secondary long-range effects. A new range of dinucleating cryptands has recently become available^{6,7} via [2+3] Schiff-base condensation of triamines with dialdehydes (generating hexaimino cryptands), and the subsequent hydrogenation of the imine function to yield octaamino derivatives. Preliminary experiments suggest that in many cases steric constraints in the hexaimino ligands prevent formation of a useful range of binuclear cryptates; however the increased flexibility inherent in the octaamino derivatives makes these more effective hosts for transition-metal ions. We have recently⁸ reported a study of the hexaimino cryptand L¹, obtained by condensation of tris(2-ethylamino)amine (tren) with terephthalaldehyde, which in the absence of non-macrocyclic (exogenous) co-ordinating ligands functions well as a host only for pairs of Ag⁺ and Cu⁺ ions. When thiocyanate ion is present, a number of M₂L(NCS)₄ complexes can be obtained, where the cation appears to utilise only two N-donors from each N₄ site.

We have now prepared the octaamino derivative, L², of L¹



and report its function as a host for first-series transition-metal ions Mn^{II} to Cu^{II}. The increased flexibility implicit in the replacement of six C=N by six C–N links permits incorporation of a range of bridging ligands, so that the dependence of magnetic interaction on the nature of the bridge can be studied. Additionally we expect the introduction of six sp³-N donors to alter the redox preferences of co-ordinated metal ions, leading to stabilisation of higher oxidation states.⁹ The investigation of binuclear complexes of polyamino cryptands such as L² is thus of interest from several points of view.

Results and Discussion

The octaamino ligand L² was prepared by tetrahydroborate reduction of disilver or dilead complexes of L¹, or in somewhat lower overall yield by direct reduction of the free ligand L¹. Complete reduction of all six imino functions was established by

* Supplementary data available (No. SUP 56901, 5 pp): magnetic susceptibility data. See Instructions for Authors, *J. Chem. Soc., Dalton Trans.*, 1992, Issue 1, pp. xx–xxv.

Non-SI units employed: G = 10⁻⁴ T, dyn = 10⁻⁵ N, cal = 4.184 J.

Table 1 Proton NMR data^a

Compound	Solvent	ν /MHz	T/K	H _A	H _C	NH	H _D	H _E
L ¹	CD ₃ OD	360	298	7.32	8.29	—	3.84 (t)	2.83 (br s)
		360	183	7.0–7.5 (m)	8.40 (s)	—	3.84 (br s)	3.4, 2.1 (br)
L ²	CD ₂ Cl ₂	360	298	6.89 (s, 4 H)	3.67 (s, 4 H)	2.0 (br s, 2 H)	2.65 (t, 4 H)	2.81 (t, 4 H)
			183	6.67 (s)	3.53 (br s)	1.55 (br s)	2.53 (br s)	2.65 (br s)
[H ₄ L ²][CF ₃ SO ₃] ₄	(CD ₃) ₂ SO	400	298	7.45 (s, 4 H)	2.80 (s, 4 H)	8.65 (br s)	4.22 (s, 4 H)	2.61 (t, 4 H)
			323	7.22 (s)	2.90 (br s)	—	3.97 (s)	2.71 (t)
[Ag ₂ L ²][CF ₃ SO ₃] ₂	CD ₃ CN	500	298	7.12 (s, 4 H)	2.78 (4 H)	2.9 (br)	3.78 ^c (4 H)	2.95 ^b
			338	7.12 (s, 4 H)	2.80 (4 H)	2.92	3.78 ^c (4 H)	3.00 (4 H)
[Cu ₂ L ²][CF ₃ SO ₃] ₂	CD ₃ CN	500	338	6.89 (4 H)	2.80	2.90 ^b	3.90, 3.65	3.28, 2.95
			298		2.80 (s)	2.85 (m)	3.95 (d), 3.53 (t)	3.35 (br t), 2.95 (d)

^a Chemical shifts δ relative to SiMe₄. ^b Overlapped. ^c Assigned on the basis of comparison with the copper(t) spectrum.

Table 2 Torsion angles (°) in [H₄L²][CF₃SO₃]₄

C(31)–C(30)–N(1)–C(10)	128.9	
C(30)–N(1)–C(10)–C(11)	–58.4	
C(31)–C(30)–N(1)–C(23*)	–99.2	
C(30)–N(1)–C(23*)–C(22*)	167.0	
C(11)–C(10)–N(1)–C(23*)	175.0	
C(10)–N(1)–C(23*)–C(22*)	–66.5	
		L ¹ ·6H ₂ O
N(1)–C(10)–C(11)–N(12)	–50.1	70.2
C(10)–C(11)–N(12)–C(13)	–167.3	–118.1
C(11)–N(12)–C(13)–C(14)	–172.9	–178.6
N(12)–C(13)–C(14)–C(15)	115.7	2.6
C(13)–C(14)–C(15)–C(16)	173.4	–177.1
C(16)–C(17)–C(20)–N(21)	–112.4	
C(17)–C(20)–N(21)–C(22)	178.4	
C(20)–N(21)–C(22)–C(23)	–153.2	
N(21)–C(22)–C(23)–N(1*)	–66.9	
N(1)–C(30)–C(31)–N(32)	–76.9	
C(30)–C(31)–N(32)–C(33)	178.6	
C(31)–N(32)–C(33)–C(34)	–49.6	
N(32)–C(33)–C(34)–C(35)	106.9	

* Symmetry operation $\frac{1}{2} - x, y, 1 - z$.

mass spectra which showed an intense $m/z = 598$ ion without trace of a peak at $m/z = 586$ corresponding to unreduced hexamine. The infrared spectrum shows a medium-intensity ν_{NH} absorption at 3231 cm^{-1} and no sign of a $\nu(\text{C}=\text{N})$ peak around 1630 cm^{-1} . Disappearance of the imino chromophore is also confirmed by the drastically reduced intensity, in the electronic spectrum, of the $\pi-\pi^*$ absorption around 240 nm, now seen as a poorly defined shoulder on the intense band at ca. 210 nm.

The ¹H NMR spectrum of L² (Table 1) at ambient temperature shows a broad, temperature-dependent resonance around δ 2.0 assigned to NH protons (time-averaged with solvent water) together with a pair of closely spaced triplets corresponding to (NH)CH₂CH₂(N) resonances and singlets at ca. δ 3.7 and 6.9 corresponding respectively to (aryl)CH₂(NH) and CH(aryl) protons. Reduction of temperature causes the aliphatic CH₂ signals to broaden, but even by 183 K (the limiting low temperature in CD₃OD) no differentiation of methylene signals into axial and equatorial resonances (as seen for L¹ by 223 K) is observed. This suggests a greater degree of conformational freedom in L² than in L¹.

Disilver and dicopper(t) azacryptates show ¹H NMR resonances at similar chemical shifts to those for the free cryptand, although it appears from the splitting pattern that the assignments are different, at least on the basis of comparison of L² and [Cu₂L²]²⁺, where the methylene coupling pattern is available to assist identification. There are significant differences in the ¹H NMR spectra of the two cryptates. In the disilver case the

resonances remain broad and unsplit down to 233 K (the limiting low temperature of the deuteroacetonitrile solvent). The dicopper(t) cryptate, on the other hand, shows an interesting fluxionality. Resonances in the δ 2.9–3.9 range develop splitting patterns below 0 °C which show them to be coupled in typical AA'BB' fashion necessitating assignment as methylene signals from the (NH)CH₂CH₂(N) assemblies. The freezing out of axial and equatorial signals for the dicopper but not the disilver cryptate indicates greater kinetic stability for the dicopper complex. [It is indeed notable that the dicopper(t) cryptate appears inert towards atmospheric oxidation; this observation also suggests the existence of kinetic barriers.⁹]

Further comparison may be made with the tetraprotonated derivative [H₄L²]⁴⁺. As expected, the most radical change is seen in the NH resonance, shifted nearly 7 ppm downfield, which is consistent with increase of positive charge on protonation together with the involvement in strong hydrogen bonding of at least some of the NH protons. The CH(aryl) signal at δ 7.3 is seen at very similar field to that⁸ of [H₂L¹]²⁺ and remains sharp down to 233 K. However, the methylene signals between δ 2.6 and 4.2 have split into several components in the weak and poorly resolved CD₃CN spectrum seen at 233 K. It appears that protonation, like co-ordination of Cu^I, is responsible for introducing some rigidity into the otherwise flexible octaamino cryptand framework.

Crystal Structure of [H₄L²][CF₃SO₃]₄.—Crystals of this tetraprotonated salt were obtained in an attempt at transmetallation of L² with manganese triflate. The structure contains cations of [H₄L²]⁴⁺ of crystallographic C₂ symmetry (Fig. 1) and two independent triflate (CF₃SO₃) anions. The dimensions in the anions are as expected. The conformation of the cation is described by the torsion angles listed in Table 2. It is apparent from these angles and from Fig. 1 that the links between the bridgehead nitrogen atoms are significantly different in conformation. This is not the case in any of the crystal structures so far determined of the ligand L¹, where there is an approximate three-fold axis coincident with the N(bridgehead)–N(bridgehead) vector (Fig. 2). The one major difference in the conformations of the links in the current molecule is located on the C–N–C–C_{aryl} torsion angles which are *trans* in two links (–172.9, 178.4°) but *gauche* (–49.6°) in the other. It is likely that this asymmetry occurs in order to facilitate intramolecular hydrogen bonding between the nitrogen atoms.

Intra- and inter-molecular hydrogen bonds are listed in Table 3. There are four independent intermolecular hydrogen bonds between NH groups on the cation and oxygen atoms of the triflates. In addition there are two intramolecular hydrogen bonds in the cation between the N(12) and N(32) atoms. The distance between the two atoms is 2.79 Å. This intramolecular hydrogen-bond pattern closes up the macrocycle and clearly is a bar to any interaction with solvent or indeed with metal ions.

The structure can be usefully compared to that found in the

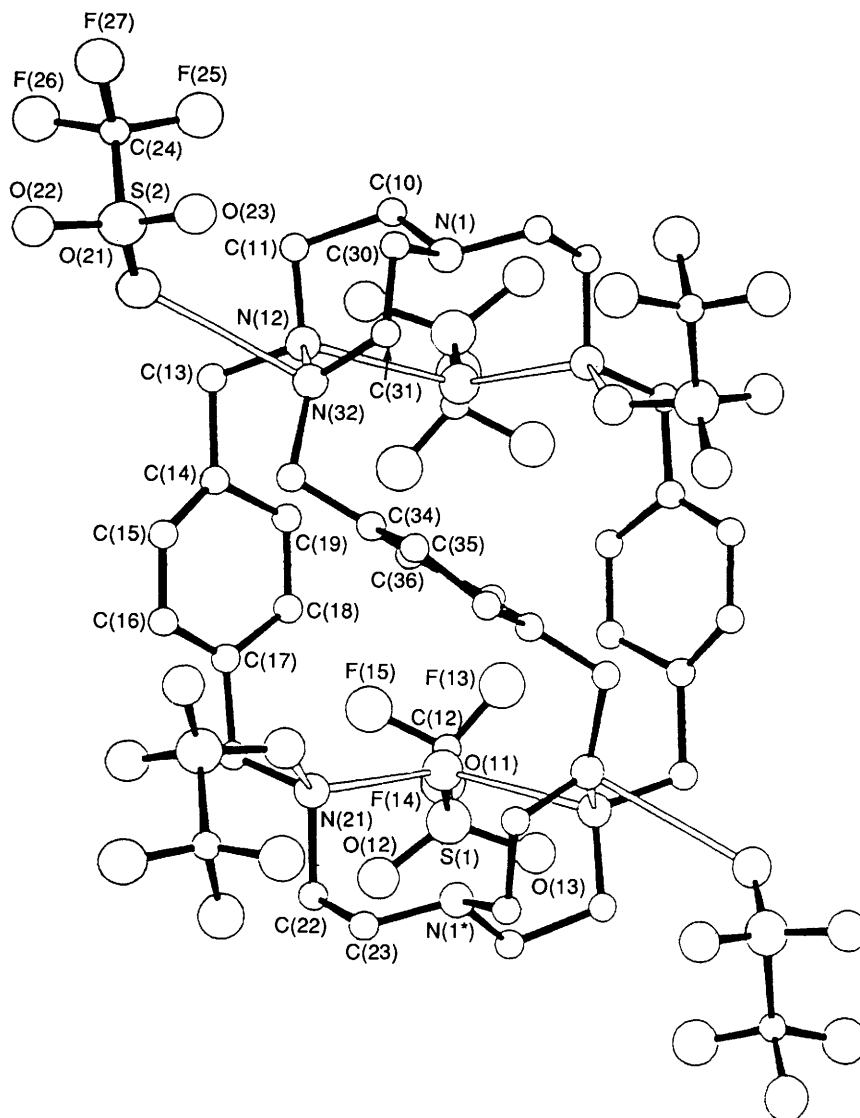


Fig. 1 General view of the crystal structure of $[H_4L^2][CF_3SO_3]_4$ showing the intra- and inter-molecular hydrogen bonds (drawn as unshaded lines); hydrogens omitted for clarity

Table 3 Hydrogen bond distances (\AA)

(a) Intermolecular

	Symmetry operation applied to oxygen	H...O	N...O
N(12)–H(121)···O(11)	$\frac{1}{2} - x, y, 1 - z$	2.04	2.98
N(21)–H(211)···O(11)	x, y, z	2.05	2.90
N(21)–H(212)···O(22)	$x, -\frac{1}{2} + y, \frac{1}{2} + z$	1.90	2.83
N(34)–H(341)···O(21)	$1 - x, \frac{1}{2} - y, \frac{1}{2} - z$	2.02	2.96

(b) Intramolecular

N(12)···N(32)	2.79
---------------	------

non-reduced ligand. For comparison the torsion angles found in the structure of $L^1 \cdot 6H_2O$ are listed in Table 2. Not surprisingly the major change is found in the N–C–C– C_{aryl} angle. This is 2.6° in L^1 because of the conjugation between the N=C bond and the phenyl ring, but is $115.7, 106.9^\circ$ in the reduced ligand. It is interesting that in this case the C(10)–C(11)–N(12)–C(13) and C(30)–C(31)–N(32)–C(33) torsion angles are -167.3 and 178.6° compared to -118.1° in the unreduced ligand. This different conformation results in a decrease in the N(bridgehead)–N(bridgehead) distance from 10.54 to 9.80 \AA .

Complex Formation.—The degree of mobility indicated by 1H NMR spectra suggests that the octaamino cryptand may be capable of accommodating guests, such as pairs of transition ions. In order to test this idea we treated L^2 with 2 equivalents of transition-metal salts, $MX_2 \cdot nH_2O$ ($M = Mn^{II}, Fe^{II}, Co^{II}, Ni^{II}, Cu^{II}$ or Cu^I ; $X = CF_3SO_3^-$ and/or ClO_4^-/NO_3^-). With Mn^{II} and Fe^{II} , in the absence of exogenous co-ordinating ions, only the tetraprotonated salt was obtained; in the case of Mn^{II} , as we have mentioned, in the form of crystals suitable for X-ray diffraction studies. With $M = Co^{II}, Ni^{II}$ or Cu^{II} , however (Table 4), dinuclear transition-metal ion complexes were obtained. In the case of Co^{II} these took the form of μ -OH dimers with both ClO_4^- and $CF_3SO_3^-$ counter ions. However with Cu^{II} the nature of the cryptate depends on counter ion, a μ -OH triperchlorate being obtained and an unbridged tetratriflate. This is in contrast to the situation with L^1 , where only the dicopper(I) cryptate was obtained in the absence of co-ordinating anion. With Ni^{II} there was no indication of μ -OH dimers, at least in the absence of deliberately added base; instead the $[Ni_2L^2]^{4+}$ salt is obtained, with some indication in the infrared spectrum of counter ion co-ordination.

The isolation of μ -OH dimers with Co^{II} and Cu^{II} is somewhat unexpected in view of the assumed largish separation of co-ordination sites. However, molecular mechanics modelling indicates that a near-linear M–O–M assembly with long M–O

Table 4 Analytical, selected infrared and magnetic data for L² complexes

Compound	Colour	Analysis (%) ^a			IR (cm ⁻¹)		μ	
		N	C	H	$\nu(\text{NH})$	$\nu(\text{N}_3^-)$ or $\nu(\text{OH}^-)$	300 K	80 K
1 [Mn ₂ L ² (N ₃)](CF ₃ SO ₃) ₃	Brown	12.4 (12.9)	38.9 (39.1)	4.3 (4.5)	3216	2186	5.76	3.97
2 [Fe ₂ L ² (N ₃)](CF ₃ SO ₃) ₃	Cream	12.8 (12.8)	39.2 (39.1)	4.4 (4.5)	3208	2151	5.27	4.91
3 [Co ₂ L ² (OH)](CF ₃ SO ₃) ₃	Green	9.2 (9.5)	39.6 (39.7)	4.7 (4.7)	3271, 3230	3585 (sh)	4.19	3.99
4 [Co ₂ L ² (OH)](ClO ₄) ₃ ·2H ₂ O	Green	10.9 (10.5)	40.4 (40.5)	5.2 (5.6)	3278, 3242	3578 (sh)	4.44	3.79
5 [Co ₂ L ² (im)](CF ₃ SO ₃) ₃	Green	11.7 (11.4)	41.5 (41.0)	4.5 (4.7)	3295, 3209		4.37	4.00
6 [Co ₂ L ² (N ₃)](CF ₃ SO ₃) ₃	Blue	12.4 (12.8)	38.4 (38.9)	4.5 (4.5)	3269, 3216	2209	4.66	4.43
7 [Ni ₂ L ²](NO ₃) ₄ ·4H ₂ O	Blue	16.5 (16.2)	41.8 (41.8)	5.9 (6.0)	3260 (sh), 3202	1478, 1453, 1380, 1324 ^b	2.90	2.71
8 [Ni ₂ L ² (N ₃)](CF ₃ SO ₃) ₃	Green	12.6 (12.5)	37.7 (37.9)	4.7 (4.4)	3270, 3217	2189	3.44	3.45
9 [Ni ₂ L ² (N ₃)](ClO ₄) ₃	Green	14.2 (14.6)	41.0 (40.9)	5.1 (5.1)	3286, 3246	2190	3.30	3.17
10 [Cu ₂ L ² (OH)](ClO ₄) ₃ ·2H ₂ O	Blue	10.4 (10.7)	40.7 (40.2)	5.2 (5.4)	3294	3578 (sh)	1.65	1.38
11 [Cu ₂ L ²](CF ₃ SO ₃) ₄	Blue	8.2 (8.5)	36.7 (36.4)	4.4 (4.1)	3222		1.98	1.53
12 [Cu ₂ L ² (im)](CF ₃ SO ₃) ₃ ·2H ₂ O	Blue	10.8 (11.0)	39.7 (39.6)	4.4 (4.6)	3304, 3229		1.66	1.37
13 [Cu ₂ L ² (N ₃)](CF ₃ SO ₃) ₃	Gold	12.4 (12.7)	38.8 (38.6)	4.4 (4.5)	3290, 3242	2200	2.15	1.87
14 [Cu ₂ L ² (N ₃)](CF ₃ SO ₃) ₃ ·2H ₂ O	Gold	12.3 (12.3)	37.3 (37.5)	3.7 (3.7)		2223	1.89	1.87
15 [Cu ₂ L ²](CF ₃ SO ₃) ₂	Cream	10.5 (10.9)	44.9 (44.6)	5.2 (5.2)	3252		<i>c</i>	
16 [Ag ₂ L ²](CF ₃ SO ₃) ₂	White	10.0 (9.5)	41.0 (40.5)	5.0 (4.3)	3272		<i>c</i>	

^a Calculated values in parentheses. ^b $\nu(\text{NO}_3^-)$. ^c Diamagnetic.

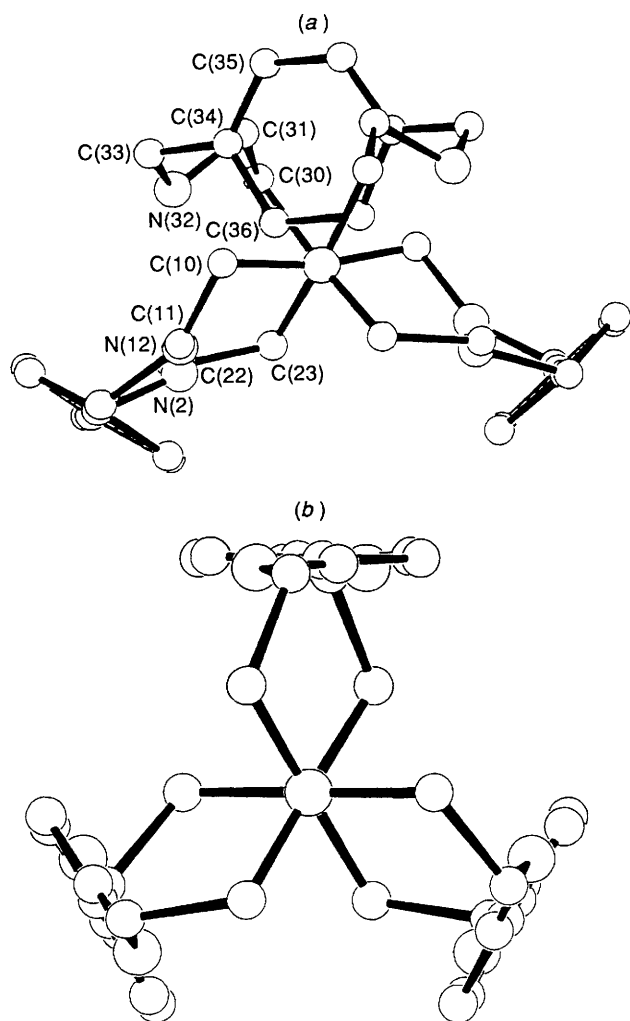


Fig. 2 The crystal structures of (a) [H₄L²]⁴⁺ and (b) L¹ in projection down the N(bridgehead)–N(bridgehead) vector. Hydrogen atoms are omitted for clarity

distances (ca. 2.48 Å) can be accommodated with little strain within this cryptand if only the three secondary amine N-donors

Table 5 Electronic spectral absorptions [in 10³ cm⁻¹ (ε/dm³ mol⁻¹ cm⁻¹)] of selected L² complexes in MeCN solution

Complex	Absorptions (10 ³ cm ⁻¹)
1	38.5 (1110)
2	31.3 (900), 10.5 (8)
3	22.8 (sh), 21.2 (130), 16.3 (sh), 15.5 (70), 12.5 (70), 7.7 (10)
4	21.0 (sh), 19.7 (190), 15.5, 15.0 (140), 13.0 (60), 7.0 (130)
5	29.4 (sh), 22.3, 20.4 (170), 16.6 (sh), 15.7 (160), 13.6 (70), 7.0 (100)
6	28.7 (171), 21.2, 20.4 (225), 15.9 (390), 15.6 (sh), 13.5 (120), 6.0 (80)
7	22.0 (90) (sh), 16.0 (50), 10.6 (60)
8	27.0 (500) (sh), 16.1 (1200), 9.7 (500)
9	24.1 (180), 16.1 (35), 9.6 (50)
10	15.4 (sh), 15.0 (200)
11	14.5 (sh) (400), 11.6 (500)
12	14.3 (430), 12.7 (480)
13	23.4 (2500), 14.1 (500), 11.0 (760)
14	21.4 (2450), 13.7 (600), 11.0 (740)

are used in co-ordination, leaving the bridgehead nitrogen unco-ordinated. The electronic spectra (Table 5) of complexes **3** and **4** do not indicate T_d co-ordination of Co^{II}, despite the (admittedly rather pale) green colour; the fairly rich moderate-intensity spectrum extending from ca. 21 000 to 5000 cm⁻¹ suggests five-co-ordination.¹⁰ This is presumably achieved *via* co-ordination of the three secondary amino N-donors, μ-OH, and counter ion or H₂O solvate. Bridging OH appears to mediate efficient antiferromagnetic interaction between high-spin cobalt(II) ions where these are in tetrahedral co-ordination (*i.e.* with ⁴A₂ ground state);¹¹ in contrast, where cobalt(II) cations in otherwise similar environments are five-co-ordinate, little interaction is observed. This is so in the present case, despite the likely near-linear arrangement of M–O–M vectors which might otherwise be expected to enhance interaction. (It must be remembered, of course, that a M–O distance greater than 2.4 Å is much longer than normally observed in a M–O–M link; it is possible that H-bonded water solvate is involved in extending this link.)

The μ-OH dicopper salt **10** shows medium-weak antiferromagnetic interaction,* with a $-2J$ value of the order of 80 cm⁻¹ and an ESR signal showing extensive, poorly resolved, hyperfine structure (at least seven lines on the $g = 2$ signal) with $A_{\parallel} = 70$ G. However, there is no large zero-field splitting, as the

* The susceptibility variation with temperature has been deposited as SUP 56901.

$g = 2$ band is not split, merely broadened. The tetratriflate salt **11** which lacks the proposed long hydroxo bridge shows $-2J = 65 \text{ cm}^{-1}$; the ESR spectrum consists of a broad single line with a hint of poorly resolved hyperfine at *ca.* 140 G, and no zero-field splitting. Evidently, even the unusually long $\mu\text{-OH}$ bonds in **10** have some role in mediating antiferromagnetic exchange between the copper(II) centres. Magnetic susceptibility measurements on the dinickel tetranitrate salt show little temperature variation over the range 200–80 K, above what would be expected for an isolated nickel(II) ion. The electronic spectrum suggests O_h co-ordination for Ni^{II} , which appears to require bridgehead nitrogen or counter-ion co-ordination; the internuclear separation may well approach the 6 Å observed in $[\text{Ag}_2\text{L}^1]^{2+}$ in this case.

Multi-atom Bridges.—As the single-atom $\mu\text{-OH}$ bridge appears to be less than ideally suited to the internuclear distance present in this cryptand, we attempted the co-ordination of two- and three-atom bridges, pyrazolate and imidazolate. We were unable to isolate well characterised pyrazolate-bridged complexes, obtaining instead $\mu\text{-OH}$ species, but imidazolate was accepted as bridging ligand by both dicobalt(II) and dicopper(II) complexes. The electronic spectrum of the dicobalt $\mu\text{-imidazolate}$ complex **5** was very similar to that of the dicobalt $\mu\text{-OH}$ species **3** and **4**, suggesting that a five-co-ordinate geometry exists also for the larger bridge. Magnetic susceptibility measurements do not indicate greater interaction *via* $\mu\text{-imidazolate}$ than $\mu\text{-OH}$, in either the dicobalt or the dicopper ($-2J = 65 \text{ cm}^{-1}$) case, but the ESR spectrum of the imidazolate-bridged dicopper complex **12** shows clear signs of thermal accessibility of a triplet state. In contrast to the dicopper $\mu\text{-OH}$ complex **10**, significant zero-field splitting ($D_{xy} = 970 \text{ G}$) exists which generates the characteristic 'triplet' pattern (Fig. 3) including a $g = 4$ 'half-band' signal with partly resolved hyperfine splitting (*ca.* 55 G) appearing with around 1/4 the intensity of that of the $g = 2$ resonance. It is not unusual with π -bridging ligands¹² to see clear indications of magnetic interaction in the ESR spectrum while magnetic moments are barely temperature-dependent. Under these circumstances, large zero-field splittings have been attributed¹³ to an excited state π -superexchange pathway, *e.g.* $d_{x,y} - \pi^*$. Certainly, given the anticipated $\text{Cu} \cdots \text{Cu}$ distance of *ca.* 5 Å, D_{dip} (the dipolar zero-field component) should not exceed¹³ 0.025 cm^{-1} , which is of the right order to explain the broadened signal in the $\mu\text{-OH}$ dimer **10**, but well below the observed zero-field splitting for **12**.

A very interesting set of properties is presented by complexes where azide ion acts as an exogenous bridge between transition-metal ions encapsulated within this ligand. The finely crystalline

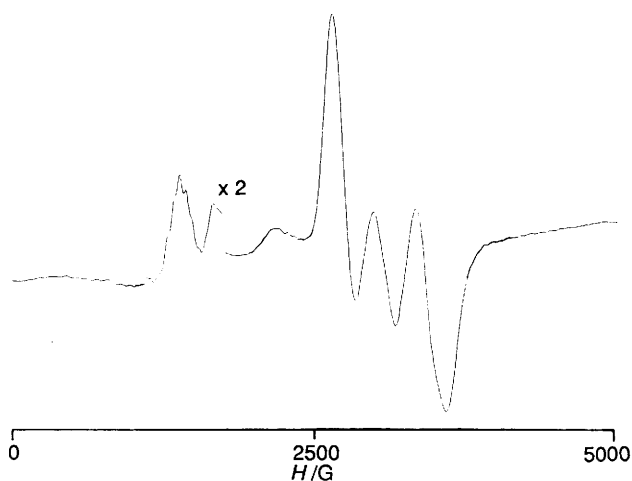


Fig. 3 X-Band ESR spectrum of complex **12** in dimethylformamide glass at 100 K

products of stoichiometry $[\text{M}_2\text{L}^2(\text{N}_3)]\text{X}_3$ ($\text{M} = \text{Mn}, \text{Fe}, \text{Co}$ or Cu ; $\text{X} = \text{CF}_3\text{SO}_3$ or ClO_4) all show $\nu_{\text{asym}}(\text{NNN})$ infrared absorption close to 2200 cm^{-1} , well above any values reported to date for co-ordinated or ionic N_3^- . Both 1,1¹⁴ and 1,3- $\mu\text{-N}_3^-$ ¹⁵ asymmetric stretching modes of co-ordinated azide normally appear within the $2000\text{--}2100 \text{ cm}^{-1}$ range, as does unco-ordinated azide. The only previous reports of azide absorption above 2200 cm^{-1} have been with aromatic azides, and attributed to the enhancement of canonical forms such as $\text{N}^- - \text{N}^+ = \text{N}$. It was thus tempting to attribute these high $\nu_{\text{asym}}(\text{N}_3^-)$ frequencies to ligand modification, *i.e.* generation of an azido-substituted aromatic by some metal-assisted process. However, available evidence militates against this suggestion; fast atom bombardment (FAB) mass spectra show medium-intensity peaks corresponding to HL^+ and/or ML^+ with no $\text{L}(\text{N}_3)$ or $\text{ML}(\text{N}_3)$ counterpart. (Although N_3^- -containing fragments are intense in the FAB mass spectrum, suggesting strong N_3^- co-ordination, N_3^- only appears in conjunction with a pair of transition ions.) Also the infrared spectrum lacks the characteristically sharp $\mu\text{-OH}$ absorption (*ca.* 3600 cm^{-1}) which stoichiometry requires should ionic azide be absent, and there is no sign of the moderate antiferromagnetic interaction which characterises $\mu\text{-OH}$ bridging between copper(II) ions in these systems.

It seemed possible that the azide ion might be sterically constrained between the cations in this macrobicyclic cyclophane in an unusual perhaps near-linear, $\text{M}-\text{NNN}-\text{M}$ geometry. This arrangement might be expected to contribute to increase of the azide stretching frequency through unusually large adjacent bond interaction arising from collinear disposition of $\text{M}-\text{N}$ and $\text{N}-\text{N}$ vectors. Such an effect may alone be sufficient to explain the high $\nu_{\text{asym}}(\text{N}_3^-)$, without invoking any increase in bond order, which could be hard to rationalize as the azide lowest unoccupied molecular orbital (LUMO) is antibonding.¹⁶ Encapsulation alone does not appear to be responsible for a high azide ν_{asym} frequency as N_3^- accommodated (*via* hydrogen bonding interactions) as guest within a polyether cryptand shows a normal¹⁷ ν_{asym} at 2085 cm^{-1} . (Our attempt to include azide within the protonated ligand L^2 by treating $[\text{H}_4\text{L}^2] - [\text{CF}_3\text{SO}_3]_4$ with excess of azide was unsuccessful.) Support for the proposal of anomalously high infrared frequencies deriving from linear $\text{M}-\text{NNN}-\text{M}$ assemblies comes from the observation of an even higher $\nu_{\text{asym}}(\text{N}_3^-)$ (2223 cm^{-1}) frequency for the dicopper $\mu\text{-azido}$ salt **14** of the related ligand L^3 which has¹⁸ a shorter cavity length.

No significant antiferromagnetic interaction appears to be transmitted through these azido bridges, except in the case of complex **1**. Here a decrease in moment from 5.8 at 300 K to 4.0 at 80 K corresponds to an exchange coupling constant, $-2J$, of 15 cm^{-1} . Compounds **2**, **6**, **8**, **9** and **14** exhibit behaviour close to the Curie law down to 80 K, and for **13** at most a weak antiferromagnetic interaction is indicated. This is in contrast to other symmetric 1,3-azido-bridged dicopper complexes with

$\text{M}-\text{NNN}-\text{M}$ geometry¹⁵ where strong antiferromagnetic interaction generates near-diamagnetism. For Cu^{II} the lack of strong interaction can be rationalized if D_{3h} symmetry applies, making d_z^2 [which is orthogonal to $^1\pi_u$, the μ -ligand highest occupied molecular orbital (HOMO)] the magnetic orbital.

The ESR spectra of dicopper $\mu\text{-azido}$ complexes, **13** and **14**, are also most unusual, particularly for apparently non-interacting copper(II) ions. The breadth of the signal (Fig. 4) testifies to existence of a very large zero-field splitting, as found in triplet ground-state molecules, but it is not easy to assign the features of the spectrum to pairs of D_z or D_{xy} components. We are presently undertaking a study of the magnetic behaviour of these and other related $\mu\text{-N}_3^-$ dicopper cryptates including susceptibility measurements and ESR spectra down to 4 K, and including simulation of spectra¹⁹ to try to understand the origin of their unusual features.

The electronic spectra of complexes **13** and **14** (Table 5) suggest D_{3h} symmetry. As for other structurally characterised

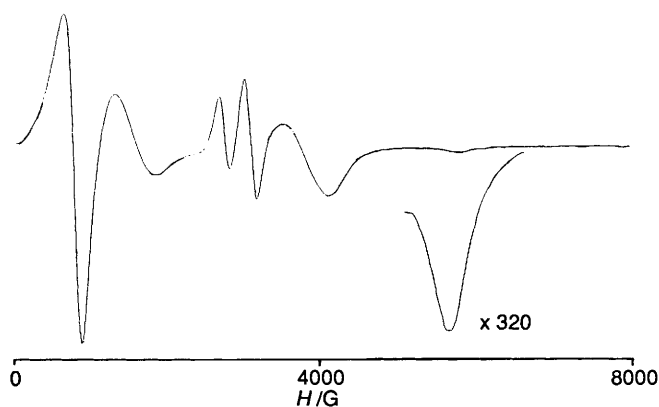


Fig. 4 X-Band ESR spectrum of complex 14 in the polycrystalline state at 7 K

trigonal-bipyramidal copper(II) complexes,²⁰ there is a pronounced splitting of the d-d absorption into two components with the more intense appearing at lower frequency, at 11 000 and 14 000 cm^{-1} . These lie close to those seen²⁰ for $[\text{Cu}(\text{tren})(\text{NH}_3)]^{2+}$, but are more intense possibly in consequence of interaction with the intense ligand to metal charge transfer (l.m.c.t.) absorption centred at ca. 21 400 cm^{-1} (467 nm). This absorption is responsible for the gold colour of the compounds, another unusual property for a 1,3- μ -azido-bridged complex.²¹ In a recent comprehensive study²² of binuclear copper(II) azide complexes it was noted that for terminal and 1,1- μ - N_3^- a single intense l.m.c.t. band appears close to 400 nm, while for 1,3- μ - N_3^- a pair of such bands, often poorly resolved and centred around 365 and 420 nm, is seen. To our knowledge, there is no other report of a band maximizing at wavelengths as long as 467 nm attributable to $\text{N}_3^- \rightarrow \text{Cu}^{\text{II}}$ charge transfer in model compounds.

In order to investigate the linearity of the M-NNN-M skeleton, crystals of $[\text{Co}_2\text{L}^2(\text{N}_3)][\text{CF}_3\text{SO}_3]_3$ (which were found to be isomorphous with [13]) were prepared and found to be trigonal with $a = 9.543$, $c = 30.12$ Å, $Z = 2$. Diffraction data were measured but were very weak and we were unable to determine the space group or solve the structure in detail. The Patterson function was consistent with $[\text{Co}_2\text{L}^2(\text{N}_3)]^{3+}$ cations lying on three-fold axes at $x = \frac{1}{3}$, $y = \frac{2}{3}$ and $x = \frac{2}{3}$, $y = \frac{1}{3}$ with the cobalt atoms 7 Å apart. This is consistent with the cobalt atoms being bridged by a linearly disposed azide anion although of course a disordered structure with an angular azide binding over three possible sites cannot be ruled out. However this seems unlikely from the estimated $\text{Co} \cdots \text{Co}$ distance. We modelled the possible structure *via* molecular mechanics using the MM2 program²³ which has been amended²⁴ to cope with metal complexes. The structure was built up using our molecular graphics system. Parameters included were taken from previous work with macrocycles.^{25,26} The ideal geometry around the cobalt atom was set at trigonal pyramidal with ideal angles of 90, 120 and 180°. Additional force-field terms specific to this structure were: bond stretching, Co-N, k_s 2.0 $\text{mdyn} \text{Å}^{-1}$, r_0 2.00 Å; N-N, k_s 3.0 $\text{mdyn} \text{Å}^{-1}$, r_0 1.20 Å; angle bending, Co-N-N, k_b 0.3 $\text{mdyn} \text{Å}^{-1} \text{rad}^{-2}$, θ_0 180.0°; N-N-N, k_b 0.3 $\text{mdyn} \text{Å}^{-1} \text{rad}^{-2}$, θ_0 180.0°. Minimization led to a structure with an energy of 37.6 kcal mol^{-1} , a linear Co-N-N-N-Co moiety (all angles within 3° of 180°) and a $\text{Co} \cdots \text{Co}$ distance of 6.46 Å. We then repeated the calculations with ideal Co-N bond lengths of 2.10 (energy 33.48 kcal mol^{-1} , $\text{Co} \cdots \text{Co}$ 6.53 Å) and 2.20 Å (energy 39.04 kcal mol^{-1} , $\text{Co} \cdots \text{Co}$ 6.63 Å). These calculations suggest that the macrocycle can accommodate the linear azide linkage without excessive strain and that the preferred $\text{Co} \cdots \text{Co}$ distance is ca. 6.5 Å which is consistent with the X-ray results. This structure is shown in Fig. 5. We searched the Cambridge Crystallographic Database for linkages of the type Co-N-N-N-Co and found only one²⁷ in which two

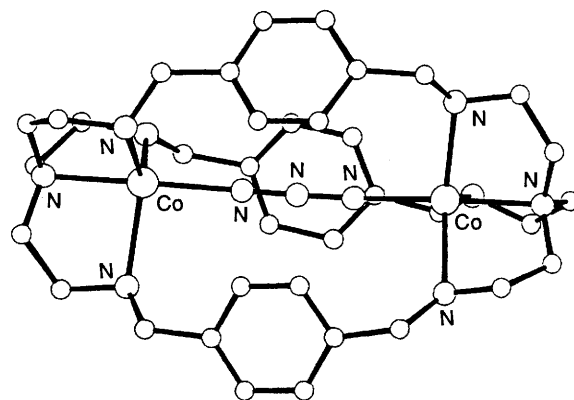


Fig. 5 Molecular mechanics model of the structure of complex 6 showing a low-energy conformation of the macrocycle with a constrained $\text{Co} \cdots \text{Co}$ distance of 6.5 Å and a 1,3 linearly bridging azide

cobalt atoms were bridged by two 1,3-azide linkages. Here the Co-N-N angles were 124.6, 139.5° and the $\text{Co} \cdots \text{Co}$ distance 5.14 Å.

The normal non-linear M-NNN-M geometry is responsible for splitting of the c.t. band through preferential overlap of the cation bonding orbitals with one of the normally degenerate pair of $1\pi_u$ azide orbitals, thus increasing the separation of ligand and metal orbitals involved in the charge-transfer process. In this case, the second orbital of the pair is barely affected by overlap with cation orbitals.

Assuming linear geometry in the present system, and the consequent orthogonality of the HOMO with the d_{z^2} cation orbitals, it would not be surprising that the c.t. band should (a) fail to split and (b) occur at relatively low energy in comparison with other μ -1,3- N_3^- complexes. The occurrence of the c.t. band at wavelengths close to 500 nm is of interest because of the observation of $\text{N}_3^- \rightarrow \text{Cu}^{\text{II}}$ charge-transfer absorption at this wavelength²² in met azido arthropod haemocyanin (*Limulus*) and also in tyrosinase. Analysis of the reasons for appearance of long-wavelength l.m.c.t. absorption in μ -azido model compounds may in time lead to elucidation of the subtle structural differences between the active sites of tyrosinase and molluscan or arthropod haemocyanin.

Experimental

Physical measurements were carried out as described in ref. 5.

Synthesis of Ligand and Complexes.—The compound L^2 was prepared by tetrahydroborate reduction of $[\text{Pb}_2\text{L}^1(\text{NCS})_4]$, synthesised as described previously.⁸ The complex (1 mmol) was suspended in ethanol (200 cm^3) and brought to reflux. A large excess of NaBH_4 was added gradually. After effervescence had ceased the black precipitate of lead was filtered off, and the filtrate evaporated to dryness and redissolved in NaOH solution. This was extracted with CHCl_3 , and the extract dried over Na_2SO_4 . Evaporation of solvent gave a cream powder in 70% yield. Mass spectrum: m/z 598 (base peak); no peaks observed at 586, 588, 590, etc.

$[\text{M}_2\text{L}^2][\text{CF}_3\text{SO}_3]_2$ ($\text{M} = \text{Cu}^{\text{I}}$ 15 or Ag^{I} 16). The ligand L^2 (0.2 mmol) was dissolved in EtOH (40 cm^3) and AgCF_3SO_3 (0.4 mmol) in MeCN (30 cm^3) was added. On slow evaporation in the dark, white crystals of $[\text{M}_2\text{L}^2][\text{CF}_3\text{SO}_3]_2$ were obtained. A procedure identical except for use of the appropriate copper(I) salt and dinitrogen protection yielded $[\text{Cu}_2\text{L}^2][\text{CF}_3\text{SO}_3]_2 \cdot 3\text{H}_2\text{O}$ 15.

$[\text{Co}_2\text{L}^2(\text{OH})]\text{X}_3 \cdot x\text{H}_2\text{O}$ ($\text{X} = \text{CF}_3\text{SO}_3^-$, $x = 0$ 3; $\text{X} = \text{ClO}_4^-$, $x = 2$, 4). The ligand L^2 (0.1 mmol) in EtOH (30 cm^3) was added to $\text{CoX}_2 \cdot 6\text{H}_2\text{O}$ (0.3 mmol) in MeCN (20 cm^3) and stirred for 30 min at 50 °C. Slow evaporation of MeCN in air

Table 6 Atomic coordinates ($\times 10^4$) with estimated standard deviations in parentheses

Atom	<i>x</i>	<i>y</i>	<i>z</i>
S(1)	2485(4)	5672(4)	6445(3)
O(11)	2545(7)	4695(8)	6156(4)
O(12)	3090(11)	5846(14)	6909(8)
O(13)	1718(17)	5803(23)	6468(12)
C(12)	2509(25)	6777(36)	6022(18)
F(13)	2036(15)	6763(24)	5546(11)
F(14)	2540(13)	7797(19)	6222(9)
F(15)	3193(13)	6827(19)	5934(8)
S(2)	4643(4)	5139(5)	1493(2)
O(21)	4787(12)	4364(16)	1135(8)
O(22)	3909(11)	5651(14)	1322(7)
O(23)	5245(15)	5862(19)	1677(10)
C(24)	4572(22)	4178(34)	2036(16)
F(25)	5269(12)	3790(15)	2277(8)
F(26)	3920(15)	3689(22)	1974(10)
F(27)	4437(11)	4913(16)	2424(7)
N(1)	2594(10)	2080(12)	3108(6)
C(10)	3064(14)	3016(20)	2948(10)
C(11)	3896(16)	3191(24)	3343(11)
N(12)	3807(9)	3267(10)	3899(5)
C(13)	4586(14)	3708(20)	4270(9)
C(14)	4549(10)	3654(12)	4870(6)
C(15)	4978(10)	3022(13)	5281(7)
C(16)	4967(14)	3091(17)	5796(9)
C(17)	4430(13)	3611(16)	5901(8)
C(18)	3897(16)	4246(22)	5493(11)
C(19)	3921(15)	4321(19)	4961(10)
C(20)	4355(13)	3564(17)	6458(9)
N(21)	3669(11)	2957(15)	6521(7)
C(22)	3645(15)	2918(21)	7135(10)
C(23)	3209(13)	1914(17)	7216(9)
C(30)	3034(13)	932(17)	3144(9)
C(31)	3099(16)	354(19)	3682(10)
N(32)	3739(9)	969(11)	4110(6)
C(33)	3891(15)	515(21)	4712(10)
C(34)	3195(10)	429(12)	4849(7)
C(35)	2821(9)	-512(11)	4898(6)
C(36)	2859(8)	1486(9)	4945(5)

gave the cryptates **3** and **4** as mid-green microcrystalline products in 80–90% yield.

$[\text{Ni}_2\text{L}^2][\text{NO}_3]_4 \cdot 4\text{H}_2\text{O}$ **7**. The ligand L^2 (0.15 mmol) and $\text{Ni}(\text{NO}_3)_2 \cdot 6\text{H}_2\text{O}$ were refluxed in EtOH–MeCN (2:1, 80 cm³) for 4 h. The solution was filtered and allowed to evaporate slowly when tiny turquoise crystals were obtained in ca. 40% yield.

$[\text{Cu}_2\text{L}^2(\text{OH})][\text{ClO}_4]_3 \cdot 2\text{H}_2\text{O}$ **10** and $[\text{Cu}_2\text{L}^2][\text{CF}_3\text{SO}_3]_4$ **11**. To L^2 (0.1 mmol) in EtOH (20 cm³) was added 0.25 mmol of the appropriate copper salt in MeCN (15 cm³). The mid-green microcrystalline precipitate was filtered off in 70–80% yield. With ClO_4^- as counter ion the stoichiometry of the product was $2\text{Cu}:3\text{ClO}_4^-$, but with CF_3SO_3^- under identical conditions it was $2\text{Cu}:4\text{CF}_3\text{SO}_3^-$.

$[\text{M}_2\text{L}^2(\text{im})][\text{CF}_3\text{SO}_3]_3 \cdot x\text{H}_2\text{O}$ ($\text{M} = \text{Co}^{\text{II}}$, $x = 0$ **5**; $\text{M} = \text{Cu}^{\text{II}}$, $x = 2$, **12**). The ligand L^2 (1 mmol) dissolved in EtOH (30 cm³) was added to $\text{M}(\text{CF}_3\text{SO}_3)_2 \cdot x\text{H}_2\text{O}$ (0.25 mmol) in MeCN (50 cm³) and imidazole (Him) (0.2 mmol) in EtOH (5 cm³) was added. On evaporation the product was obtained as fine green crystals in ca. 50% yield.

$[\text{M}_2\text{L}^2(\text{N}_3)]\text{X}_3$ ($\text{X} = \text{CF}_3\text{SO}_3^-$, $\text{M} = \text{Mn}^{\text{II}}$ **1**, Fe^{II} **2**, Co^{II} **6**, Ni^{II} **8** or Cu^{II} **13**; $\text{X} = \text{ClO}_4^-$, $\text{M} = \text{Ni}^{\text{II}}$ **9**). The ligand L^2 (1 mmol) dissolved in EtOH (30 cm³) was added to $\text{M}(\text{CF}_3\text{SO}_3)_2 \cdot x\text{H}_2\text{O}$ (0.25 mmol) in MeCN (50 cm³), and finally NaN_3 (0.1 mmol) dissolved in 3 drops of water and EtOH (5 cm³) was added with vigorous stirring. On evaporation small crystals of product were obtained in ca. 60–70% yield. The L^3 complex **14** was made by an analogous procedure, substituting L^3 (ref. 18) for L^2 .

Safety Note.—Although there are possible safety hazards in working with azides, no explosions were experienced while working with these systems. It would probably be unwise, however, to increase the scale of the preparations. Testing a tiny quantity on a microspatula in a flame showed explosive tendency with the azide perchlorate **9** so this compound should be treated with great care and handled in very small quantity.

X-Ray Crystallography for $[\text{H}_4\text{L}^2][\text{CF}_3\text{SO}_3]_4$.—*Crystal data.* $\text{C}_{40}\text{H}_{56}\text{F}_{12}\text{N}_8\text{O}_{12}\text{S}_4$, $M = 1198.7$, monoclinic, space group $A2/a$ (non-standard setting of no. 15), $a = 18.185(16)$, $b = 11.928(10)$, $c = 25.634(17)$ Å, $\beta = 106.8(1)$, $U = 5321.8$ Å³, $D_c = 1.49$ g cm⁻³, $Z = 4$, $\lambda = 0.7107$ Å, $\mu = 2.88$ cm⁻¹, $F(000) = 2480$.

A crystal of approximate size $0.20 \times 0.20 \times 0.20$ mm was set up to rotate about the a axis on a Stoe Stadi2 diffractometer and data were collected *via* variable-width ω scan. Background counts were for 20 s and a scan rate of 0.0333 s⁻¹ was applied to a width of $(1.5 + \sin \mu / \tan \theta)$. 2169 Independent reflections were measured with a 2θ maximum of 50° of which 977 with $I > 2\sigma(I)$ were used in subsequent refinement. The crystal diffracted weakly but no deterioration was observed during the data collection. The structure was determined by direct methods. The cation had crystallographically imposed C_2 symmetry. The anions had high thermal motion and were possibly disordered although we were unable to refine a satisfactory model. The S–C and C–F distances were constrained to be equivalent. Owing to the poor quality of the data, all atoms were refined isotropically with the exception of the sulfurs in the anions which were refined anisotropically. Hydrogen atoms bonded to carbon were included in calculated positions and refined isotropically. The tetrapositive cation has four additional protons to be distributed around six nitrogen atoms. It was assumed that the bridgehead nitrogen atoms would not be protonated, particularly as geometry calculations showed that such protons would not participate in any hydrogen bonds. Thus two of the three independent nitrogen atoms must be attached to two hydrogen atoms, the other nitrogen atom to only one. In order to position these hydrogen atoms, we looked at the Fourier difference map and considered possible hydrogen bonds. Atom N(12) was allocated two hydrogen atoms both of which were hydrogen bonded to triflate oxygen atoms. However N(21) and N(32) were only 2.79 Å apart and calculations showed that, if both were allocated two hydrogen atoms, two such atoms would be only 1.02 Å apart. Therefore each were allocated one hydrogen atom, which is hydrogen bonded to a triflate oxygen atom. It can be assumed that an additional hydrogen atom is shared between the two atoms but we were unable to locate its position on either nitrogen atom in the Fourier map and it was not included in the refinement. The other hydrogen atoms bonded to nitrogen were included in fixed positions. A weighting scheme of the form $w = 1/[\sigma^2(F) + 0.003F^2]$ was employed. The final R value was 0.078 ($R' = 0.082$). Calculations were carried out using SHELX 76²⁸ together with some of our own programs on the Amdahl 5870 computer at the University of Reading. In the final cycles of refinement no shift/error ratio was greater than 0.1σ . In the final Fourier difference maps the maximum and minimum peaks were 0.45 and -0.35 e Å⁻³. Atomic coordinates are given in Table 6.

Additional material available from the Cambridge Crystallographic Data Centre comprises H-atom coordinates, thermal parameters and remaining bond lengths and angles.

Acknowledgements

We thank the Department of Education, Northern Ireland and the Open University Research Committee for support (to J. H. and D. J. M.). We are grateful to the SERC for access to services (Mass Spectrometry, Swansea, and High-field NMR, Warwick) and for part-funding the Faraday balance. Thanks are also due

to Mr. A. Johans, University of Reading, for assistance in obtaining the crystallographic data.

References

- 1 J. M. Lehn, *Pure Appl. Chem.*, 1980, **52**, 2441; 1977, **49**, 857.
- 2 R. J. Motekaitis, A. E. Martell, J.-M. Lehn and E. Watanabe, *Inorg. Chem.*, 1982, **21**, 4253.
- 3 Y. Agnus, *Copper Co-ordination Chemistry: Biochemical and Inorganic Perspectives*, eds K. Karlin and J. Zubieta, Adenine Press, New York, 1983, p. 371.
- 4 M. G. B. Drew, F. S. Esho, S. M. Nelson, V. McKee and J. Nelson, *J. Chem. Soc., Dalton Trans.*, 1982, 1837.
- 5 M. G. B. Drew, P. Yates, C. J. Harding, D. McDowell, C. Stevenson, S. Raghunathan and J. Nelson, *J. Chem. Soc., Dalton Trans.*, 1990, 2521.
- 6 J. Jazwinski, J. M. Lehn, D. Lilenbaum, R. Ziessel, J. Guilheim and C. Pascard, *J. Chem. Soc., Chem. Commun.*, 1987, 1691.
- 7 D. McDowell and J. Nelson, *Tetrahedron Lett.*, 1988, **29**, 385.
- 8 M. G. B. Drew, J. Hunter, D. Marrs and J. Nelson, *J. Chem. Soc., Dalton Trans.*, 1992, 11.
- 9 M. McCann, J. Nelson and L. Qin, *Inorg. Biochem.*, in the press.
- 10 A. B. P. Lever, *Inorganic Electronic Spectroscopy*, Elsevier, New York, 1968.
- 11 M. G. B. Drew, F. S. Esho, A. Lavery and S. M. Nelson, *J. Chem. Soc., Dalton Trans.*, 1984, 545.
- 12 A. Bencini, D. Gatteschi, J. Reedijk and C. Zanchini, *Inorg. Chem.*, 1985, **24**, 207.
- 13 D. N. Hendrickson and T. Felthouse, *Inorg. Chem.*, 1978, **17**, 444 and refs. therein.
- 14 M. G. B. Drew, F. S. Esho and S. M. Nelson, *Inorg. Chim. Acta*, 1983, **83**, L269.
- 15 V. McKee, J. V. Dagdigian, R. Bau and C. A. Reed, *J. Am. Chem. Soc.*, 1981, **103**, 7000, Y. Agnus, R. Louis and R. Weiss, *J. Am. Chem. Soc.*, 1979, **101**, 3381.
- 16 S. D. Peyerunhoff and R. J. Buenker, *J. Chem. Phys.*, 1967, **47**, 1953.
- 17 B. Dietrich, J. Guilheim, J. M. Lehn, C. Pascard and E. Sonveaux, *Helv. Chim. Acta*, 1984, **67**, 91.
- 18 V. McKee, W. T. Robinson, D. McDowell and J. Nelson, *Tetrahedron Lett.*, 1989, 7453.
- 19 P. Rieger, J. Nelson and C. Harding, unpublished work.
- 20 M. Duggan, N. Ray, B. Hathaway, G. Tomlinson, P. Brint and K. Pelin, *J. Chem. Soc., Dalton Trans.*, 1980, 1342 and refs. therein.
- 21 T. H. Sorrell, in *Biological and Inorganic Copper Chemistry*, eds K. Karlin and J. Zubieta, Adenine Press, New York, 1985.
- 22 J. E. Pate, P. K. Ross, T. J. Thamann, C. A. Reed, K. D. Karlin, T. N. Sorrell and E. H. Solomon, *J. Am. Chem. Soc.*, 1989, **111**, 5198.
- 23 MM2, N. L. Allinger and Y. H. Yuh, Quantum Chemistry Program Exchange Program No. 423, Indiana University Chemistry Department, IN.
- 24 M. G. B. Drew, S. Hollis and P. C. Yates, *J. Chem. Soc., Dalton Trans.*, 1985, 1829.
- 25 W. G. Haanstra, W. A. J. W. van der Donk, W. L. Driessen, J. Reedijk, J. S. Wood and M. G. B. Drew, *J. Chem. Soc., Dalton Trans.*, 1990, 3123.
- 26 M. G. B. Drew and P. C. Yates, *J. Chem. Soc., Dalton Trans.*, 1987, 2563.
- 27 A. Bencini, C. A. Ghilardi, S. Midollini and A. Orlandini, *Inorg. Chem.*, 1989, **28**, 1958.
- 28 G. M. Sheldrick, SHELX 76, Package for Crystal Structure Determination, University of Cambridge, 1976.

Received 8th May 1992; Paper 2/02369E